

Further Evaluations of STAP Tests in Compound-Gaussian Radar Clutter

¹J.H. Michels, ²M. Rangaswamy, and ¹B. Himed

¹AFRL/SNRT, 26 Electronic Parkway Rome, NY 13441

²ARCON Corporation, Waltham, MA 02451-1080

Abstract—The performance of a parametric space-time adaptive processing (STAP) method is presented here. Specifically, we consider signal detection in additive disturbance containing compound-Gaussian clutter plus additive Gaussian thermal white noise. Performance is compared to the normalized adaptive matched filter and the Kelly GLRT receiver using simulated and measured data. We focus on the issues of detection and false alarm probabilities, constant false alarm rate (CFAR), robustness with respect to clutter texture power variations, and reduced training data support.

I. INTRODUCTION

This paper undertakes a performance comparison of several candidate space-time adaptive processing (STAP) algorithms in compound-Gaussian clutter for airborne radar applications. The STAP problem is equivalent to hypothesis testing on a complex (baseband) measurement (test data) vector $\mathbf{x} \in C^{JN}$ with J channels and N time pulses. Typically, \mathbf{x} contains an unwanted additive disturbance \mathbf{d} with unknown covariance matrix \mathbf{R}_d and may contain a desired signal $a\mathbf{e}$ with unknown complex amplitude, a , and known signal steering vector \mathbf{e} . The binary detection problem is to select between hypothesis $H_0 : a = 0$ and $H_1 : a \neq 0$ given a single realization of \mathbf{x} .

Current research [1–10] is addressing the detection problem wherein \mathbf{d} contains partially correlated clutter described by a product model [11]. Here, the clutter is modeled as a Gaussian process with random power variations (scale changes) over range. This model is the basis of the spherically invariant random process (SIRP)(or compound-Gaussian) clutter model, which includes the Weibull and K-distributions as special cases.

In [6, 12, 13] the optimal processor for detecting a rank one signal in SIRP clutter was shown to be equivalent to a matched filter compared to a data dependent threshold. With a simple normalization, this test can be cast in the form of the normalized matched filter (NMF) test compared to a data dependent threshold, the calculation of which requires knowledge of the underlying clutter probability density function (PDF). Determination of the clutter PDF imposes onerous training data requirements. Consequently, ad hoc methods have been popular in recent studies [7–10]. A popular

ad-hoc method is the NMF test compared to a data independent threshold, which was independently derived in [7, 8].

The work of [14] (and references therein) considered an invariance framework for hypothesis testing in Gaussian noise having a covariance matrix with known structure but unknown level. Interestingly, the test statistic reported in [14] is identical to the NMF of [7, 8]. The work of [14] also extended the NMF test to allow for an unknown noise covariance matrix and unknown scaling, η^2 , denoting the ratio of the test and training data variances. We refer to this test as the normalized adaptive matched filter (NAMF). The invariance principle of [14] (and references therein), and perform constant false alarm rate (CFAR), applies only when all the training data vectors are scaled identically [10].

In SIRP clutter, however, each training data vector realization is scaled by a different random parameter. Although the NAMF has no known optimality properties for SIRP clutter, it has the important feature of minimizing dependence upon texture power. Some performance results of the NAMF in SIRP clutter are presented in [7, 8].

Multichannel model-based (i.e., parametric) methods for target detection and estimation in clutter are described in [2–4, 9, 10, 15–17]. In particular, a model-based STAP method called the non-Gaussian parametric adaptive matched filter (NG-PAMF), requiring knowledge of the underlying clutter statistics was first proposed in [3].

In this paper, the performance of the normalized parametric adaptive matched filter (N-PAMF) [10, 18] is evaluated and compared with that of several candidate STAP algorithms. Its form is the model-based approximation of the NAMF. Statistical equivalence of the N-PAMF test to the NG-PAMF test was shown in [10]. However, unlike the NG-PAMF, the N-PAMF test requires no ‘a priori’ knowledge of the disturbance statistics [10]. This feature is important in real-time applications where such information is lacking. Robustness of P_d over a broad range of K-distribution shape parameters (α) ranging from Gaussian ($\alpha = \infty$) to high-tailed PDF ($\alpha = 0.1$) is presented here. These considerations enable assessments of CFAR performance with respect to the amplitude probability density function (APDF)

DISTRIBUTION STATEMENT A

Approved for Public Release
Distribution Unlimited

20020807 233

associated with clutter texture variations. Finally, we examine performance versus data support size used for disturbance estimation. This issue is of considerable importance in applications where training data support is limited.

II. THE CLUTTER MODEL

Clutter observed in a single channel admits a representation of the form

$$c_k(n) = v_k(n)g_k(n) \quad (1)$$

where a complex-Gaussian process $g_k(n)$ (speckle component) corresponding to time n and range cell k is modulated by a statistically independent non-negative process $v_k(n)$ (texture component). Frequently, $v_k(n)$ is approximated as a random variable V over k , but constant over time if it has long temporal coherence. Thus, (1) reduces to the representation theorem [11] for an SIRP and is given by

$$c_k(n) = v_k g_k(n). \quad (2)$$

For the multichannel problem, the clutter in each of the J channels is given by (2). The PDF of V , $f_V(v)$, is defined to be the characteristic PDF of the SIRP. The amplitude of $c_k(n)$ is K-distributed for Generalized-Chi distributed $f_V(v)$ and includes the Gaussian model ($\alpha = \infty$) as a special case. The disturbance \mathbf{d} contains partially correlated clutter \mathbf{c} modeled by a K-distributed amplitude, with PDF

$$f_R(r) = \frac{\beta^{\alpha+1} r^\alpha}{2^{\alpha-1} \Gamma(\alpha)} K_{\alpha-1}(\beta r) \quad r \geq 0, \beta, \alpha > 0 \quad (3)$$

where β and α are the distribution scale and shape parameters, respectively, $K_\nu(\cdot)$ is the modified Bessel function of the second kind of order ν , and $\Gamma(\cdot)$ is the Eulero-Gamma function. Small values of α result in heavy-tails for the PDF of (3). From (2), the clutter covariance matrix is $\mathbf{R}_c = \mathbf{R}_g E(V^2)$ where $\mathbf{R}_g \in C^{JN \times JN}$ is the covariance of the Gaussian (speckle) component and $E(V^2)$ relates to the texture power.

In practice, \mathbf{R}_d is unknown, and must be estimated from a signal-free $JN \times K$ secondary data matrix, \mathbf{Z} , whose columns are assumed to be statistically independent and identically distributed (iid) as the test data. For Gaussian disturbance, the maximum likelihood (ML) estimator is the sample matrix $\hat{\mathbf{R}}_d = \mathbf{Z}\mathbf{Z}^H/K$. However, $\hat{\mathbf{R}}_d$ is not the ML estimate for compound-Gaussian clutter.

III. TEST STATISTIC DESCRIPTIONS

We now consider several non-adaptive and adaptive detection test statistics in this section.

A. Non-Adaptive Test Statistics

For known \mathbf{R}_d , the optimal test for detecting a rank one signal in Gaussian interference is given by

$$\Lambda_{MF} = \frac{|\mathbf{e}^H \mathbf{R}_d^{-1} \mathbf{x}|^2}{\mathbf{e}^H \mathbf{R}_d^{-1} \mathbf{e}} \stackrel{H_1}{>} \stackrel{H_0}{<} \lambda_{MF}. \quad (4)$$

In some instances, the test data vector can have a covariance matrix $\eta^2 \mathbf{R}_d$, where η^2 is an unknown level. The phase invariant matched filter (PI-MF) test for these problems is expressed as [14]

$$\Lambda_{PIMF} = \frac{|\mathbf{e}^H \mathbf{R}_d^{-1} \mathbf{x}|^2}{\eta^2 \mathbf{e}^H \mathbf{R}_d^{-1} \mathbf{e}} \stackrel{H_1}{>} \stackrel{H_0}{<} \lambda_{PIMF} \quad (5)$$

where \mathbf{e} and \mathbf{x} are the concatenated $JN \times 1$ signal ‘search’ steering and data vectors, respectively. The inner product of whitened vectors $\mathbf{b} = \mathbf{R}_d^{-\frac{1}{2}} \mathbf{x}$ and $\mathbf{f} = \mathbf{R}_d^{-\frac{1}{2}} \mathbf{e}$ is the matched filtering operation. Although (5) does not require knowledge of signal phase, it does require knowledge of the level η^2 to be CFAR. The optimal test for this problem is the NMF test [14] given by

$$\Lambda_{NMF} = \frac{|\mathbf{e}^H \mathbf{R}_d^{-1} \mathbf{x}|^2}{[\mathbf{e}^H \mathbf{R}_d^{-1} \mathbf{e}] [\mathbf{x}^H \mathbf{R}_d^{-1} \mathbf{x}]} \stackrel{H_1}{>} \stackrel{H_0}{<} \lambda_{NMF}. \quad (6)$$

The test statistic of (6) is simply the squared magnitude of the inner product of the vectors \mathbf{f} and \mathbf{b} normalized by their squared norms, so that $0 \leq \lambda_{NMF} \leq 1$.

B. Adaptive Test Statistics

For the adaptive problem, $\hat{\mathbf{R}}_d$ replaces \mathbf{R}_d . Consequently, the adaptive version of the test of (4) denoted as the AMF is given by

$$\Lambda_{AMF} = \frac{|\mathbf{e}^H \hat{\mathbf{R}}_d^{-1} \mathbf{x}|^2}{\mathbf{e}^H \hat{\mathbf{R}}_d^{-1} \mathbf{e}} \stackrel{H_1}{>} \stackrel{H_0}{<} \lambda_{AMF}. \quad (7)$$

Observe that Λ_{AMF} is simply the adaptive version of Λ_{MF} . For the special case of $\eta = 1$, this test was developed independently in [19,20] where its CFAR behavior was noted. This property is lost when $\eta \neq 1$.

The adaptive version of the test of (6) is given by

$$\Lambda_{NAMF} = \frac{|\mathbf{e}^H \hat{\mathbf{R}}_d^{-1} \mathbf{x}|^2}{[\mathbf{e}^H \hat{\mathbf{R}}_d^{-1} \mathbf{e}] [\mathbf{x}^H \hat{\mathbf{R}}_d^{-1} \mathbf{x}]} \stackrel{H_1}{>} \stackrel{H_0}{<} \lambda_{NAMF}. \quad (8)$$

Another adaptive detection test known as the Kelly GLRT [21] is expressed as

$$\Lambda_{GLRT} = \frac{|\mathbf{e}^H \hat{\mathbf{R}}_d^{-1} \mathbf{x}|^2}{[\mathbf{e}^H \hat{\mathbf{R}}_d^{-1} \mathbf{e}] [1 + \frac{\mathbf{x}^H \hat{\mathbf{R}}_d^{-1} \mathbf{x}}{K}]} \stackrel{H_1}{>} \stackrel{H_0}{<} K \lambda_{GLRT} \quad (9)$$

where $0 \leq \lambda_{GLRT} \leq 1$. For $K \rightarrow \infty$, the tests of (7) and (9) converge to the test of (4), whereas the test of (8) converges to that of (6).

In this paper, we consider the performance of the tests of (7)- (9) in compound-Gaussian clutter. No optimality or CFAR claims of these tests can be made for the case of SIRP disturbance.

C. Model-Based STAP Tests

For multichannel model-based methods [15], the whitening operation is performed using prediction error filters (PEF) involving time series or state space architectures. We define $\mathbf{y}_p(n)$ as the $J \times 1$ vector error residual output of a P^{th} -order multichannel linear filter. For a multi-channel (vector) autoregressive model, a tapped delay line architecture is used where the P^{th} order filter coefficients, $\hat{\mathbf{A}}(k)$, are estimated from \mathbf{Z} using a multichannel parameter estimation algorithm. These $J \times J$ matrix coefficients provide a succinct description of the spatio-temporal disturbance correlation. Specifically,

$$\begin{aligned} \mathbf{y}_p(n) &= \hat{\mathbf{D}}_0^{-\frac{1}{2}} \hat{\mathbf{L}}_0^{-1} \mathbf{u}_p(n) \\ &= \hat{\mathbf{D}}_0^{-\frac{1}{2}} \hat{\mathbf{L}}_0^{-1} [\mathbf{x}(n|H_1) + \sum_{k=1}^P \hat{\mathbf{A}}(k) \mathbf{x}(n-k+P|H_1)] \\ n &= 0, 1, \dots, N-P-1 \end{aligned} \quad (10)$$

where (10) implicitly defines the temporally whitened $J \times 1$ error residual $\mathbf{u}_p(n)$, with covariance Σ_u . In practice, Σ_u is unknown and the estimation algorithms produce its estimate $\hat{\Sigma}_u$. However, this paper employs $\hat{\Sigma}_u$ obtained by averaging the outer products of $\mathbf{u}_p(n)$, where $\mathbf{u}_p(n)$ results from a transformation of the secondary data by the prediction error filter with fixed $\hat{\mathbf{A}}(k)$. The \mathbf{LDL}^H decomposition of $\hat{\Sigma}_u$ yields $(\hat{\mathbf{L}}_0, \hat{\mathbf{D}}_0)$ which are used to spatially whiten $\mathbf{u}_p(n)$ [15]. Finally, $\mathbf{y}_p(n)$ is obtained by a transformation of $\mathbf{x}(n)$ by the multichannel prediction error filter with coefficients $(\hat{\mathbf{L}}_0, \hat{\mathbf{D}}_0)$ and $\hat{\mathbf{A}}(k)$ as denoted in (10). Similarly, the transformed steering vector $\mathbf{s}(n)$ is obtained by sequencing the sequential form of the ‘search’ steering vector $\mathbf{e}(n)$ through the PEF [3, 16]. The normalized parametric adaptive matched filter (N-PAMF) [10, 18] is now defined as

$$\Lambda_{N-PAMF} = \frac{\left| \sum_{n=0}^{N-P-1} \mathbf{s}^H(n) \mathbf{y}_p(n) \right|^2}{\left[\sum_{n=0}^{N-P-1} \mathbf{s}^H(n) \mathbf{s}(n) \right] \left[\sum_{n=0}^{N-P-1} \mathbf{y}_p^H(n) \mathbf{y}_p(n) \right]} \quad (11)$$

A related parametric adaptive matched filter (PAMF) test was first derived in [3] for Gaussian disturbance.

The PAMF test is identical to (11) but excludes the second bracketed denominator term. In [16], several estimation algorithms are considered in the PAMF implementation for Gaussian disturbance. In this paper the multichannel least squares method is used for filter parameter estimation.

IV. ANALYTICAL RESULTS

The probability of false alarm and probability of detection for NMF operating in compound-Gaussian clutter (without background white noise) are given by [9]

$$P_{fa-NMF} = P(\Lambda_{NMF} > \lambda_{NMF}|H_0) = (1 - \lambda_{NMF})^{JN-1} \quad (12)$$

$$\begin{aligned} P_{d-NMF} &= 1 - (1 - \lambda_{NMF})^{JN-1} \\ &\times \sum_{k=1}^{JN-1} b_k \left(\frac{\lambda_{NMF}}{1 - \lambda_{NMF}} \right)^k g_k[A^2(1 - \lambda_{NMF})] \end{aligned} \quad (13)$$

where $g(.)$ is defined in [9] and $b_k = \frac{\Gamma(JN)}{\Gamma(k+1)\Gamma(JN-k)}$.

The expressions for P_{fa} and P_d for the NAMF operating in Gaussian clutter are given by [9]

$$P_{fa-NAMF} = \int_0^1 \frac{f_\Gamma(\gamma)}{[1 + (1 - \gamma)\lambda_{NAMF}]^L} d\gamma \quad (14)$$

$$\begin{aligned} P_{d-NAMF} &= 1 - \int_0^1 \frac{1}{[1 + (1 - \gamma)\lambda_{NAMF}]^L} \\ &\times \sum_{m=1}^L \binom{L}{m} \eta^m (1 - \gamma)^m \\ &\times [1 - \text{gammainc} \left(\frac{A(1 - \gamma)}{1 + (1 - \gamma)\lambda_{NAMF}}, m \right)] f_\Gamma(\gamma) d\gamma \end{aligned} \quad (15)$$

where Γ , $\text{gammainc}(.)$ and $f_\Gamma(\gamma)$ are defined in [9].

Corresponding P_{fa} and P_d expressions for the NAMF operating in SIRP clutter are difficult to derive. This is due to the fact that the ML estimate of the SIRP covariance matrix is not available in closed form [22]. Hence, the NAMF PDF cannot be determined analytically.

The P_{fa} and P_d expressions for the N-PAMF and PAMF operating in both Gaussian and non-Gaussian clutter scenarios are lacking since the analysis becomes mathematically intractable. Consequently, performance evaluation of these methods is carried out by Monte-Carlo techniques.

V. PERFORMANCE RESULTS

Performance is now presented for the detectors described above. Probability of detection (P_d) is computed for a P_{fa} of 0.01 via 100,000 Monte-Carlo trials using a physical model of an airborne radar scenario [4]. The target signal is located at a normalized Doppler frequency $f_{dt} = 0.15$ (unless otherwise

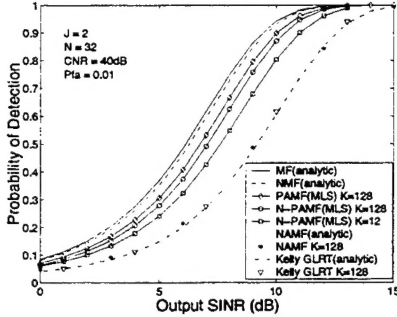


Fig. 1. P_d versus output SINR in Gaussian disturbance

stated) and azimuth $\phi = 0$. The clutter ridge is located along the normalized angle-Doppler plane diagonal with a 40 dB (per pulse, per channel) clutter-to-noise ratio(CNR). The one-lag clutter temporal correlation parameter [15] is 0.999. Disturbance correlation estimates are obtained using K secondary data cells. The output signal-to-interference plus noise ratio (SINR) is defined as $SINR = |a|^2 \mathbf{e}^H \mathbf{R}_d^{-1} \mathbf{e}$. All performance results are obtained with compound-Gaussian clutter plus additive thermal white noise.

Figure 1 shows P_d versus output SINR for Gaussian disturbance with $\eta^2 = 1$. Shown here are analytical P_d plots for the MF and NMF with known \mathbf{R}_d . The analytical NAMF P_d curve is also shown for K=128. Monte-Carlo generated P_d results for the PAMF(MLS), N-PAMF(MLS), NAMF, and Kelly GLRT are depicted. Performance of the Kelly GLRT and the NAMF are indistinguishable for this example. Note that the N-PAMF method with $P = 3$, nearly achieves the NMF performance for low sample support size K=12. Singularity of $\hat{\mathbf{R}}_d$ for K=12 precludes implementation of the AMF, NAMF, and Kelly GLRT. Figures 2 and 3 display P_d versus output SINR for the NMF, NAMF, N-PAMF(MLS), Kelly GLRT and AMF receivers for clutter processes with shape parameters $\alpha = 0.5$ and $\alpha = 0.1$, respectively. Observe the robust behavior of the N-PAMF, NAMF, Kelly GLRT in compound-Gaussian clutter. The Kelly GLRT outperforms the NAMF at high SINRs, whereas this condition reverses at low SINRs. Figure 4 plots P_d versus the clutter shape parameter α at output SINR=6dB with α ranging from 0.1 to 1,000. For the K-distribution, $\alpha > 4$ approximates the Gaussian case. The results reveal the robustness of the N-PAMF and NAMF tests over a wide range of shape parameters. However, the N-PAMF(MLS) shows superior performance approaching that of the NMF. Performance of the PAMF and AMF degrade in heavy-tailed compound-Gaussian clutter.

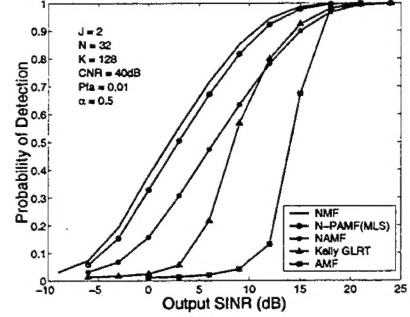


Fig. 2. P_d versus SINR in K-distributed Clutter $\alpha = 0.5$

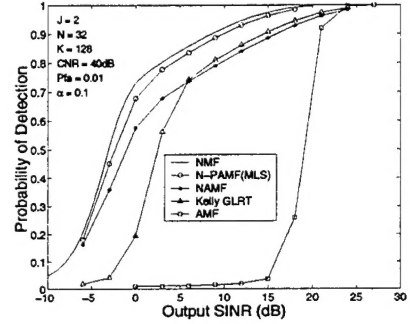


Fig. 3. P_d versus output SINR in K-distributed Clutter $\alpha = 0.1$

ter. However, for $\alpha > 100$ (Gaussian region), they incur no performance degradation. Figure 5 shows P_{fa} versus shape parameter α with each test statistic threshold held fixed to obtain $P_{fa} = 0.01$ for Gaussian disturbance ($\alpha = \infty$). A significant increase in P_{fa} for the NAMF and Kelly GLRT confirms their lack of CFAR with respect to texture variations. Figures 6, 7, and 8 depict plots of P_{fa} versus threshold for the Kelly GLRT, NAMF, and N-PAMF, respectively, for several K-distribution shape parameter values. The curves for the N-PAMF exhibit much lower variability compared to the Kelly GLRT and NAMF, reflecting a robust CFAR performance with respect to the texture PDF. Figures 9 and 10 plot the test statistic vs range cell using data from the Air Force Research Laboratory (AFRL) Multichannel Airborne Radar Measurement (MCARM) program with an inserted target signal at range bin index 310. Specifically, data corresponding to acquisition '220' from flight '5' cycle 'e' is used in the examples presented here. For these results, we use $J=8$ and $N=32$. We define the performance measure Ψ_1 as the ratio of the test statistic at the test cell to the mean of the test statistics formed from adjacent cells, and Ψ_2 as the ratio of the test statistic at the test cell

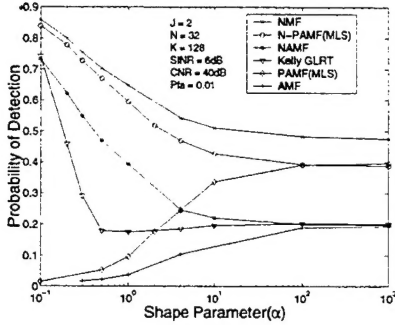


Fig. 4. P_d versus shape parameter (α)

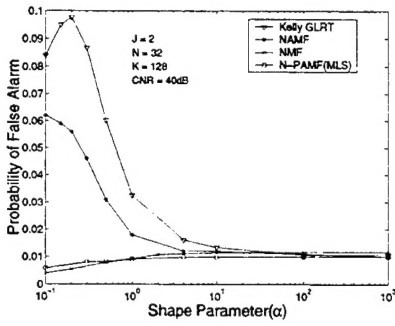


Fig. 5. P_{fa} versus clutter shape parameter(α):fixed threshold

to the highest test statistic formed from adjacent cells. Figure 9 plots the test statistics for the NAMF with $K=512$ and N-PAMF(MLS) ($P=2$) with $K=16$. Figure 10 plots the test statistics for the Kelly GLRT with $K=512$ and the N-PAMF (MLS)($P=2$) with $K=16$. Table 1 shows Ψ_1 and Ψ_2 for several values of K and P using the N-PAMF. Note that the N-PAMF with $P=2$ and $K=16$ provides the best performance for this scenario. In this instance, large sample support does not result in improved performance due to training data nonhomogeneity.

	P	Ψ_1 (dB)	Ψ_2 (dB)
NAMF ($K=512$)		16.2	7.45
Kelly GLRT ($K=512$)		16.71	8.03
N-PAMF ($K=512$)	4	19.3	12.3
N-PAMF ($K=32$)	3	22.1	14.7
N-PAMF ($K=16$)	3	21.6	15.2
N-PAMF ($K=32$)	2	21.8	11.3
N-PAMF ($K=16$)	2	22.4	14.7

Table 1: Values of Ψ_1 and Ψ_2 for the N-PAMF(MLS), NAMF, and Kelly GLRT

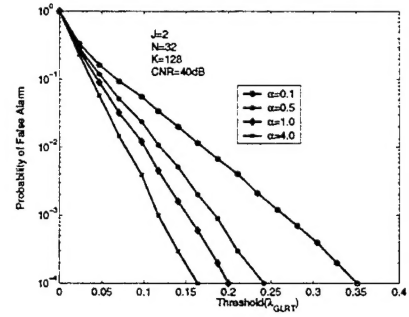


Fig. 6. P_{fa} versus threshold (λ_{GLRT}) for the Kelly GLRT

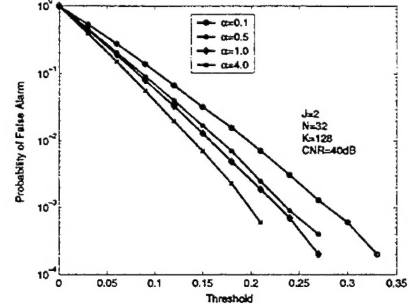


Fig. 7. P_{fa} versus threshold for the NAMF

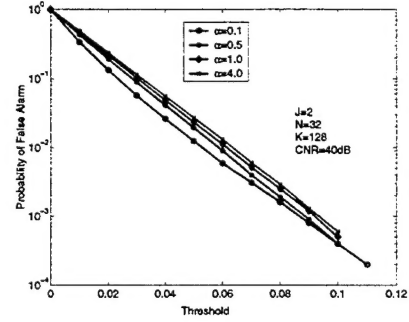


Fig. 8. P_{fa} versus threshold for the N-PAMF

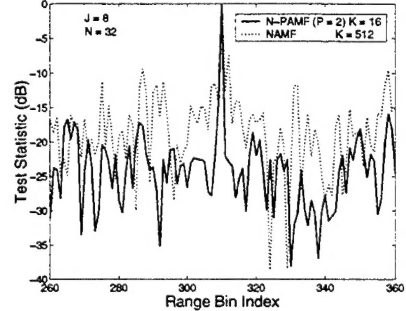


Fig. 9. Test Statistic versus Range

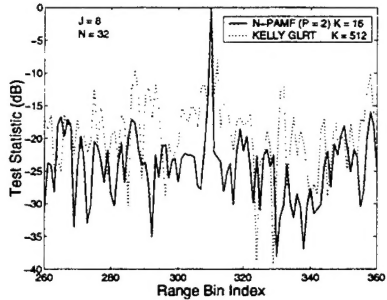


Fig. 10. Test Statistic versus Range

VI. SUMMARY AND FUTURE RESEARCH

In this paper, we have evaluated the performance of the N-PAMF, NAMF, and Kelly GLRT in compound-Gaussian clutter disturbance. The robust detection performance of these methods was shown over a wide range of clutter texture power variations (shape parameters) for K-distributed clutter processes. Performance of the N-PAMF was found to be close to the NMF. Next, the CFAR behavior was considered by observing the detection threshold variations with respect to shape parameter. Additionally, we demonstrate the robustness of the N-PAMF method with respect to small sample support size K (secondary data cells) used to estimate the disturbance correlation. This property is significant in operational scenarios involving range varying nonstationary clutter which severely limits the availability of representative training data. Examples with real data illustrate the potential for considerable performance improvement of the N-PAMF over the NAMF and Kelly GLRT.

VII. ACKNOWLEDGMENTS

This work was supported by the Air Force Office of Scientific Research (AFOSR) and in-house research efforts at AFRL/SNRT.

REFERENCES

- [1] M. Rangaswamy, D. Weiner, and J. Michels, "On the multichannel innovations based detection algorithm for correlated non-Gaussian random processes," in *Proceedings of twenty-seventh Asilomar Conference on Signals, Systems and Computers*, (Pacific Grove, CA), 1993.
- [2] M. Rangaswamy, J. Michels, and D. Weiner, "Multichannel detection for correlated non-Gaussian random processes based on innovations," *IEEE Trans. on Signal Processing*, vol. **SP-43**, pp. 1915–1922, 1995.
- [3] M. Rangaswamy and J. Michels, "A Parametric Multichannel Detection Algorithm For Correlated Non-Gaussian Random Processes," in *Proceedings of the IEEE National Radar Conference*, (Syracuse, NY), 1997.
- [4] J. Michels, T. Tsao, B. Himed, and M. Rangaswamy, "Space-Time Adaptive Processing (STAP) in Airborne Radar Applications," in *Proceedings of the IASTED Conference on Signal Processing and Communications*, (Canary Islands, Spain), 1998.
- [5] K. Gerlach, "Spatially distributed target detection in non-Gaussian clutter," *IEEE Trans. on Aerospace and Electronic Systems*, vol. **35**, no.3, pp. 1058–1069, 1999.
- [6] M. Rangaswamy and J. H. Michels, "Performance Analysis of Space-Time Adaptive Processing Methods in Non-Gaussian Radar Clutter Backgrounds," in *Proceedings of the International Conference on Radar Systems*, (Brest, France), 1999.
- [7] E. Conte, M. Lops, and G. Ricci, "Asymptotically optimum radar detection in compound-Gaussian clutter," *IEEE Trans. on Aerospace and Electronic Systems*, vol. **AES-31**, pp. 617–625, 1995.
- [8] F. Gini, "Sub-optimum coherent radar detection in a mixture of K-distributed and Gaussian clutter," *IEE Proc.F, Radar, Sonar and Navigation*, vol. **144** (1), pp. 39–48, 1997.
- [9] J. Michels, M. Rangaswamy, and B. Himed, "Performance of STAP tests in compound Gaussian clutter," in *Proceedings of the First IEEE Workshop on Sensor Array and Multichannel Processing (SAM-2000)*, (Cambridge, MA), 2000.
- [10] J. Michels, B. Himed, and M. Rangaswamy, "Performance of STAP tests in Gaussian and Compound-Gaussian Clutter," *Digital Signal Processing*, vol. **10**, no.4, pp. 309–324, 2000.
- [11] K. Yao, "A representation theorem and its applications to spherically invariant random processes," *IEEE Trans. on Information Theory*, vol. **IT-19**, pp. 600–608, 1973.
- [12] F. Gini, M. Greco, and A. Farina, "Clairvoyant and adaptive signal detection in non-Gaussian clutter: A data-dependent threshold interpretation," *IEEE Trans. on Signal Processing*, vol. **47**, no.6, pp. 1522–1531, 1999.
- [13] K. Sangston, F. Gini, M. Greco, and A. Farina, "Structures for radar detection in compound Gaussian clutter," *IEEE Trans. on Aerospace and Electronic Systems*, vol. **35**, no.2, pp. 445–458, 1999.
- [14] S. Kraut, L. L. Scharf, and L. McWhorter, "Adaptive subspace detectors," *IEEE Trans. on Signal Processing*, vol. **49**, pp. 1–16, 2001.
- [15] J. Michels, *Multichannel Detection Using the Discrete-Time Model-Based Innovations Approach*. PhD thesis, Syracuse University, 1991.
- [16] J. Roman, M. Rangaswamy, D. Davis, Q. Zhang, B. Himed, and J. Michels, "Parametric adaptive matched filter for airborne radar applications," *IEEE Trans. on Aerospace and Electronic Systems*, vol. **36**, no.2, pp. 677–692, 2000.
- [17] A. Swindlehurst and P. Stoica, "Maximum Likelihood Methods in Radar Array Signal Processing," *Proceedings of the IEEE*, vol. **86**, No. 2, pp. 421–441, 1998.
- [18] J. Michels, "Space-time adaptive processing (STAP) in Gaussian and non-Gaussian airborne radar clutter," in *Adaptive Radar Clutter Suppression Workshop*, <http://siwg.eris.dera.gov.uk/signal/aspc/>, (DERA, Malvern, U.K.), July 14 1999.
- [19] L. Cai and H. Wang, "On adaptive filtering with the CFAR feature and its performance sensitivity to non-Gaussian interference," in *Proceedings of the 24th Annual conference on Information Sciences and Systems*, (Princeton, NJ), pp. 558–563, 1990.
- [20] F. Robey, D. Fuhrmann, E. Kelly, and R. Nitzberg, "A CFAR adaptive matched filter detector," *IEEE Trans. on Aerospace and Electronic Systems*, vol. **AES-28**, pp. 208–216, 1992.
- [21] E. Kelly, "An adaptive detection algorithm," *IEEE Trans. on Aerospace and Electronic Systems*, vol. **AES-22**, pp. 115–127, 1986.
- [22] M. Rangaswamy and J. H. Michels, "Adaptive Processing in Non-Gaussian Noise Backgrounds," in *Proceedings of the Ninth IEEE Workshop on Statistical Signal and Array Processing*, (Portland, OR), 1998.